

Cascade Models of Synaptically Stored Memories

Stefano Fusi,¹ Patrick J. Drew,² and L.F. Abbott^{2,*}

¹Institute of Physiology

University of Bern

Bühlplatz 5

CH-3012, Bern

Switzerland

²Volen Center and

Department of Biology

Brandeis University

Waltham, Massachusetts 02454

Summary

Storing memories of ongoing, everyday experiences requires a high degree of plasticity, but retaining these memories demands protection against changes induced by further activity and experience. Models in which memories are stored through switch-like transitions in synaptic efficacy are good at storing but bad at retaining memories if these transitions are likely, and they are poor at storage but good at retention if they are unlikely. We construct and study a model in which each synapse has a cascade of states with different levels of plasticity, connected by meta-plastic transitions. This cascade model combines high levels of memory storage with long retention times and significantly outperforms alternative models. As a result, we suggest that memory storage requires synapses with multiple states exhibiting dynamics over a wide range of timescales, and we suggest experimental tests of this hypothesis.

Introduction

The remarkable ability of humans and other animals to retain memories of everyday occurrences imposes a severe challenge for any model of memory. Whereas single-trial learning under stressful or exceptionally rewarding conditions can rely on special modulatory influences, memory for the commonplace must arise from processes that continuously modify neural circuits. The capacity of human memory in word and picture recognition tasks is remarkably large and long lasting (Nickerson, 1965; Shepard, 1967; Standing et al., 1970; Standing, 1973; Simons, 1996), but forgetting does occur and appears to follow power-law rather than exponential dynamics (Wixted and Ebbesen, 1991, 1997). How can these features be explained within the context of our understanding of mechanisms of activity-dependent plasticity?

The idea that synaptic plasticity is the basic mechanism of memory is as old as our knowledge of synapses, and it has dominated neuroscience research for decades. The standard metaphor for memory storage in neuroscience is that of a synaptic switch; a perma-

nent change that occurs within a set of synapses due to the neuronal activity evoked by an experience. Memory recall corresponds to detection of this change when modified neural circuits are later reactivated. This essentially static view of memory is the basis of virtually all models of memory (see Amit, 1989; Hertz et al., 1991), and it pervades the experimental field as well. But memory is clearly not a static phenomenon, and studies of synaptic plasticity reveal a rich set of complex, coupled, and highly dynamic phenomena, not a simple switch-like structure (Bliss and Collingridge, 1993; Brecht and Nicoll, 2003). Furthermore, it can be shown mathematically that, for many types of memory, permanently switching synaptic efficacy is an inefficient mechanism that does not lead to permanent memory storage (Amit and Fusi, 1992, 1994; Fusi, 2002; see below).

The main challenge in building models of long-lasting memory, especially in cases where new experiences are continually generating new memories, is protecting the memory trace from the ravages of ongoing activity, not from the ravages of time. Evidence suggests that forgetting is a consequence of ongoing activity and acquisition of new experiences, not merely a passive decay of the memory trace (Jenkins and Dallenbach, 1924; Brown and Xiang, 1998; Wixted and Ebbesen, 1991, 1997). Similarly, spontaneous activity can reverse LTP, a process known as “depotentialiation,” both in vitro (Staubli and Lynch, 1990; Larson et al., 1993; O’Dell and Kandel, 1994; Xiao et al., 1996; Zhou et al., 2003) and in vivo (Barnes, 1979; Ahissar et al., 1992; Fu et al., 2002; Zhou et al., 2003; Xu et al., 1998; Manahan-Vaughan and Braunevel, 1999; Abraham et al., 2002), where depotentialiation has been shown to be an activity- and NMDA-dependent process (Villarreal et al., 2002). A mechanism such as LTP that produces persistent changes in synaptic efficacy in a silent slice preparation cannot maintain a permanent memory trace in vivo if the synaptic enhancements that represent that trace are obliterated by further plasticity (Grossberg, 1982).

To protect memories from being corrupted by ongoing activity and by the storage of new memories, which is the primary challenge in constructing realistic models of memory, we propose going beyond the switch analogy to construct models of memory based on the types of dynamic biochemical cascades that are ubiquitous in biological systems and, in particular, are associated with synaptic plasticity. Cascades provide a mechanism for getting around the limited capacity of switch-based models of memory. Furthermore, cascade models provide a framework for understanding and describing the enormous complexity of synaptic plasticity and its molecular underpinnings (Brecht and Nicoll, 2003; Sanes and Lichtman, 1999). Indeed, an important feature of the proposed model is that memory performance relies on the complexity of the cascade. Finally, and perhaps most importantly, cascade models introduce rich temporal dynamics, including power-law

*Correspondence: abbott@brandeis.edu

rather than exponential forgetting, into memory modeling.

Results

General Approach

In this paper, we discuss how memories are stored through synapse modification, and we evaluate how stored memory traces degrade over time due to ongoing plasticity. To do this, we take an “ideal observer” approach, which means that we imagine that we have access to the values of the strengths of all the synapses relevant to a particular memory trace. Of course, we do not imagine that neural circuits detect memory traces by directly monitoring the values of synaptic strengths as we do. Instead, activity in these circuits is highly sensitive to synaptic strengths, allowing modifications in network activity arising from memory-induced synaptic changes to be detected. By assuming we have access to the values of synaptic strengths and by using general signal-detection theory, we derive an upper limit on memory lifetimes. Given the remarkable capacity of animal and human memory, it seems likely that neural circuits perform quite close to this optimal level.

The memory phenomenon that we are exploring is the recognition that an unremarkable, everyday experience has occurred previously. Recognition is a useful measure of memory retention because it only implies that some trace of the memory, in virtually any form, remains in the neural circuit. Lifetimes and storage capacities are longer for recognition than for full memory recall (Bogacz et al., 2001), so our results can be viewed as an upper bound for full recall of memories. To make our calculations tractable, we assume that the memories being stored evoke synaptic plasticity in apparently random patterns, which means that there are no correlations between the activity-dependent modifications at different synapses. We also assume that the everyday memories we are discussing are not subject to various protective (Grossberg, 1982) or re-storage mechanisms (see, for example, Walker et al., 2003) that might apply for memories of exceptional experiences.

We study a system that is continuously storing new memories of everyday occurrences, and our approach is to select one of these at random and track it over time. By selecting a particular memory to track, we are also selecting a particular set of synapses; all the synapses that are modified when that particular memory is stored initially. It is important to note that the memory we are tracking is not special or different in any way, so that our results for this one particular memory apply equally to all the memories being stored.

The recognition “signal” corresponding to the memory trace being tracked is contained in the changes in synaptic strengths induced by its initial storage. Following memory storage, we assume that the synapses we are tracking are subject to further plasticity due to ongoing activity and to the storage of other memories. The resulting continual modification of memory-storing synapses introduces fluctuations in the value of the memory signal that represent a “noise” above which the memory signal must be detected. We characterize

the size of this noise by computing the standard deviation of the fluctuations in the memory signal. Because the system comes to equilibrium fairly rapidly and because storage of the tracked memory causes only a minor perturbation on the system as a whole, this noise level can be treated as constant. The signal, on the other hand, changes with time due to ongoing plasticity that degrades the stored memory by modifying the strengths of the synapses representing it, thereby reducing the magnitude of the memory signal.

Our approach to computing memory lifetimes is to compare the signal corresponding to the stored memory to the general level of noise caused by ongoing fluctuations in the strengths of the synapses being tracked. We define the memory lifetime, which is the maximum time over which a memory can be detected, as the time at which the ratio of signal to noise diminishes to 1. We are interested primarily in how the memory lifetime depends on various parameters, in particular the number of synapses. For this purpose, it doesn't matter if we set the critical signal-to-noise ratio at 1 or 0.1 or any other fixed value—the same functional dependences are obtained.

In all the models we discuss, it is important to distinguish the rate at which candidate plasticity events occur from the rate at which actual synaptic modifications occur. A candidate plasticity event is the occurrence of a pattern of activity that could potentially lead to synaptic modification; for example, in spike timing-dependent plasticity, a pair of pre- and postsynaptic action potentials occurring within the appropriate time window. We assume that such candidate events occur randomly at an average rate r . The probability that one of these candidate events satisfied the conditions that can lead to strengthening of a synapse is given by f_+ , and the probability that it is a candidate for synaptic weakening is given by $f_- = 1 - f_+$. Within the models we study, a parameter q (or a set of such parameters) determines the probability that a candidate plasticity event actually generates a change of synaptic efficacy. Thus, candidate events for synaptic strengthening occur at a rate f_+r , and these lead to actual strengthening of the synapse at a rate qf_+r . Similarly, candidate events for synaptic weakening occur at a rate f_-r , and these lead to actual weakening of the synapse at a rate qf_-r .

Ongoing “background” plasticity, related to chance plasticity events and storage of memories other than the one being tracked, is characterized by random modifications of individual synapses in the tracked set at the rates given at the end of the previous paragraph. On the other hand, storage of the tracked memory corresponds to modification of all the synapses being tracked at the same time with probability q . During storage of the tracked memory, we assume that a fraction f_+ of the synapses are strengthened with probability q and the remaining fraction $f_- = 1 - f_+$ are weakened with probability q . In the binary models we discuss below, q takes a fixed value. In the cascade models we subsequently introduce, the value of q depends on the state of the synapse, and thus it can change over time.

The rate of ongoing plasticity, denoted by r , is a critical parameter in our calculations. This corresponds to the average rate of candidate plasticity events in the relevant memory-storage circuits during normal experi-

ence. The value of r is not known, so we leave it as a free parameter in our formulae and results. We can, however, provide a rough estimate of its value. Modification of synapses due to spike timing-dependent plasticity can occur whenever pre- and postsynaptic neurons fire within about 50 ms of each other (see, for example, [Bi and Poo, 1998](#)). Taking background firing rates of 2 Hz and assuming pre- and postsynaptic firing is random and uncorrelated, such coincidences would occur at a rate of about $r = 0.2$ Hz, or once every 5 s.

In summary, our general approach is to compute signal-to-noise ratios of memory traces stored in synaptic modifications. We use two quantities to characterize the quality of memory performance. The first is the signal-to-noise ratio immediately after memory storage (called the initial signal-to-noise ratio and denoted by S_0/N_0), which is a measure of the flexibility of the system for storing new memories. The second is the memory lifetime (denoted by t_{\max}), which is the time following storage when the signal corresponding to a particular memory trace becomes equal to the noise due to ongoing synaptic modification arising from spontaneous activity and the storage of other memories. We first provide calculations of these quantities based on general considerations. In this initial discussion, we will not be concerned with numerical coefficients, rather we concentrate on how the initial signal-to-noise ratio and memory lifetime depend on critical factors such as the number of synapses being used to store the memory. We then analyze a specific model in more detail on the basis of computer simulations.

Memory Lifetimes

We begin our analysis of memory lifetimes by assuming a binary model in which synapses have only two levels of efficacy: weak and strong. The probability that a synapse makes a transition between its two levels of efficacy when a candidate plasticity event occurs is given by the transition probability q discussed above. There is some experimental evidence for binary synapses ([Petersen et al., 1998](#)), but the problems we discuss and solutions we propose using binary models generalize to the nonbinary case as well.

When a memory is stored through the systematic modification of a population of N_{syn} binary synapses, the initial memory trace that results, which we call the “signal,” is proportional to the number of synapses that have been modified, $\text{Signal} \sim qN_{\text{syn}}$. Further plasticity due to ongoing activity and the storage of additional memories will modify some of the synapses that are maintaining this trace, thereby degrading it. If the rate of ongoing plasticity events is r and the probability that these produce a change in the synapse is q , the probability that a particular synapse is not modified over a time interval t is $\exp(-qrt)$. Thus, a memory trace established at time zero will be represented by a degraded signal at time t , $\text{Signal} \sim qN_{\text{syn}} \exp(-qrt)$. A second effect of ongoing plasticity is to introduce continuous fluctuations in synaptic strength, producing “noise” with an amplitude proportional to the square root of the number of synapses, $\text{Noise} \sim \sqrt{N_{\text{syn}}}$ (assuming independent fluctuations). With this level of noise and $\text{Signal} \sim qN_{\text{syn}} \exp(-qrt)$, the signal-to-noise ratio goes to

1 at a time $t_{\max} \sim \ln(q\sqrt{N_{\text{syn}}}) / (qr)$. This is an extremely disconcerting result ([Amit and Fusi, 1992, 1994; Fusi, 2002](#)). One of the main attractions of using synapses as the repositories of memory is that there are so many of them. The fact that memory lifetimes only grow logarithmically as a function of the number of synapses used to store the memory eliminates this advantage because the logarithm is such a slowly increasing function. If the ongoing plasticity rate is 5 s and $q = 1$, memories stored using a million synapses will only last about 30 s, and memories stored using a billion synapses about a minute.

The short lifetime for memories stored by binary synapses with $q = 1$ is due to the deleterious effects of ongoing plasticity, not to any intrinsic decay mechanism at the synapse. One remedy that has been proposed is to reduce the rate at which synapses change their strength by reducing q ([Amit and Fusi, 1992, 1994; Fusi, 2002; Tsodyks, 1990](#)). If q is severely reduced, the memory lifetime can be increased significantly until a maximum value of $t_{\max} \sim \sqrt{N_{\text{syn}}} / (er)$ is reached when $q = e / \sqrt{N_{\text{syn}}}$ [where $e = \exp(1)$]. Thus, allowing the transition probability to vary as a function of the number of synapses being used to store the memory, rather than being fixed, would, at first sight, appear to solve the problem of the logarithmic dependence of memory lifetime on synapse number. However, there are several problems associated with this solution. First, it requires the probability of synaptic modification to be very low, and this causes the size of the memory signal (which is proportional to q) to be extremely small even immediately after a memory is stored. Indeed, for the value $q = e / \sqrt{N_{\text{syn}}}$ given above, which maximizes the memory lifetime, the initial signal-to-noise ratio is only $S_0/N_0 = e$. This is not much larger than 1, which disagrees with our experience that memories are quite vivid immediately after storage and then tend to fade away, and it is independent of the number of synapses being used. Thus, in this scheme, allowing the memory lifetime to take advantage of the large number of synapses through the square-root dependence in the maximal value $t_{\max} \sim \sqrt{N_{\text{syn}}} / (er)$ has the unfortunate side effect of keeping the initial signal-to-noise ratio from taking a similar advantage.

The blue curve in [Figure 1](#) indicates the relationship between the initial signal-to-noise ratio of the memory trace and the memory lifetime (in units of $1/r$) for the binary model. The initial signal-to-noise ratio decreases roughly inversely in relation to the memory lifetime and is quite small near the point where the memory lifetime reaches its maximum. Thus, it is impossible to achieve both long memory lifetimes and strong initial memory traces in this type of model. In addition, achieving long memory lifetimes requires that the transition probability be quite accurately adjusted as a function of the number of synapses used to store the memory, something that may be difficult to achieve biophysically.

The discussion above applies to binary models in which synaptic strengths take two values. It is possible to improve memory performance by introducing multiple levels of synaptic strength if the processes of synaptic potentiation and depression are accurately balanced against each other ([Amit and Fusi, 1994; Fusi, 2002](#)). However, as we will show in [Figure 6](#), even small

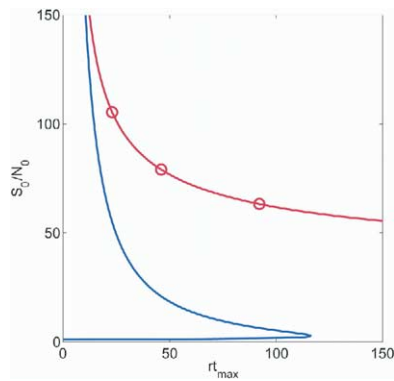


Figure 1. Initial Signal-to-Noise Ratio as a Function of Memory Lifetime

The initial signal-to-noise ratio of a memory trace for a memory stored using 10^5 synapses plotted against the memory lifetime (in units of 1 over the rate of candidate plasticity events). The blue curve is for a binary model with synaptic modification occurring with a probability q that varies along the curve. The red line applies to the cascade model described in this paper. The open circles correspond to different numbers of elements in the cascade; the red line is drawn only to guide the eye. The two curves have been normalized so that the binary model with $q = 1$ gives the same result as the $n = 1$ cascade model to which it is identical.

imbalances between the effects of synaptic strengthening and weakening spoil this result. Thus, the improvement relies on fine-tuning. Furthermore, this solution increases the numerical coefficient that relates t_{\max} to $\ln(\sqrt{N_{\text{syn}}})$, but it does not address the fundamental problem that the memory lifetime only increases as a logarithmic function of the number of synapse.

Depending on the value of q , memory lifetimes in the binary model are, at best, proportional to the square root of the number of synapses and, at worse, almost independent of the number of synapses. Memory lifetimes in traditional neural network associative memory models (Amit, 1989; Hertz et al., 1991) applied to recognition memory are proportional to the number of synapses (Bogacz et al., 2001). Unfortunately, this is achieved at the expense of allowing synaptic strengths to increase or decrease without bound, even allowing them to become negative. (In some cases, bounds are imposed on synaptic strengths after all the memories are loaded into the network, which is equivalent to imposing biophysical reality only at the end of an animal's lifetime.) A consequence of this unphysical assumption is that there is no equilibrium distribution for the strengths of the synapses in these models. In any biophysically plausible model, an equilibrium distribution of synaptic strengths must exist, and the limits on memory lifetime that we are discussing apply to such models (Amit and Fusi, 1992, 1994; Fusi, 2002). Other mechanisms for prolonging memory lifetimes, such as halting memory storage at a certain memory capacity (Willshaw, 1969) or using knowledge of stored memories to protect them (Grossberg, 1982) are not applicable to the case of ongoing memory storage that we are considering.

In summary, memory storage and memory retention impose conflicting requirements on a neural system. Storing

new memories quickly and faithfully requires a high degree of plasticity, but the best way to lock in those memories is to eliminate plasticity. In defining optimality for a memory system, we face a related dilemma, deciding how to balance the conflicting requirements of a large initial signal-to-noise ratio for the memory trace and a long memory lifetime. We see this clearly in the binary model. The initial signal-to-noise ratio in the binary model is maximized when the transition probability is set to 1. This makes the initial signal-to-noise ratio proportional to the square root of the number of synapses being used, $S_0 / N_0 \propto \sqrt{N_{\text{syn}}}$, but at the expense of a memory lifetime that only grows logarithmically with the number of synapses, $t_{\max} \propto \ln(\sqrt{N_{\text{syn}}})$. An alternative strategy is to maximize the memory lifetime by choosing a small transition probability. This makes the memory lifetime proportional to the square root of the number of synapses, $t_{\max} \propto \sqrt{N_{\text{syn}}}$, but at the expense of an initial signal-to-noise ratio that is independent of the number of synapses. A natural question that arises from these results is whether a model exists that combines the best of both of these alternatives, that is, a memory lifetime and initial signal-to-noise ratio that are both proportional to $\sqrt{N_{\text{syn}}}$. As we will see, the cascade model we propose comes very close (to within a logarithmic factor) of achieving this goal.

Power-Law Forgetting

The solution we propose for improving memory performance is to modify the logarithmic dependence of the memory lifetime on the number of synapses. Recall from the derivation that this logarithm arose from the exponential decay of the memory trace. The situation could be improved significantly if the memory trace had a power-law rather than exponential decay (as experiments suggest it should, see Wixted and Ebbesen, 1991, 1997). In this case, the signal would satisfy (for large times) $\text{Signal} \sim N_{\text{syn}} t^{-k}$ for some value of k . With the noise still satisfying $\text{Noise} \sim \sqrt{N_{\text{syn}}}$, we find that the signal-to-noise ratio goes to 1 at a time $t_{\max} \sim (N_{\text{syn}})^{1/(2k)}$. This represents a dramatic improvement over the logarithmic dependence found above, especially if k is small. Forgetting curves are fit by k values less than 1 (Wixted and Ebbesen, 1991 & 1997), suggesting that memory lifetimes can grow faster than the square root of the number of synapses, which is much faster than logarithmically. Assume, for example, that $k = 3/4$ (the value that we obtain in the model discussed below), so that $1/(2k) = 2/3$. Then, for an ongoing plasticity rate of 5 s, memories stored using a million synapses will last for about 14 hr, and memories stored using a billion synapses for almost 60 days. These are reasonable lifetimes for the types of everyday, unremarkable memories that we are studying. Thus, power-law forgetting provides a mechanism for solving the dilemma of memory lifetimes that do not take advantage of the large number of available synapses. The rest of this paper will describe how a model with power-law forgetting can be constructed and explore its consequences.

The Cascade Model

It is well known that power-law dynamics can be generated by the interactions of multiple exponential pro-

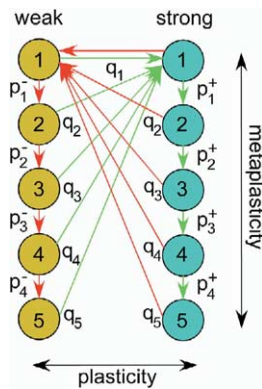


Figure 2. Schematic of a Cascade Model of Synaptic Plasticity
There are two levels of synaptic strength, weak (brown) and strong (turquoise), denoted by + and -. Associated with each of these strengths is a cascade of n states ($n = 5$ in this example). Transitions between state i of the \pm cascade and state 1 of the opposite cascade take place with probability q_i (arrows pointing up and to the left or right), corresponding to conventional synaptic plasticity. Transitions with probabilities p_i^\pm link the states within the \pm cascades (downward arrows), corresponding to metaplasticity.

cesses characterized by widely ranging time scales (Anderson, 2001). This is the approach we follow in constructing a model with power-law forgetting. In synaptic terms, this requires combining conventional synaptic plasticity with metaplasticity (Abraham and Bear, 1996; Fischer et al., 1997), which corresponds to transitions of a synapse between states characterized by different degrees of plasticity rather than different synaptic strengths.

The structure of the cascade model of synaptic plasticity is shown in Figure 2. Throughout, we consider models that have two levels of synaptic strength, weak and strong, denoted by + and - symbols. (Note that weak does not imply a zero strength synapse, but rather one that is weaker than what we call a strong synapse.) The model could be extended to multiple strength levels, but we consider the simplest form because it corresponds to the binary case considered above and because it represents a worst-case scenario. Each of the synaptic strengths is associated with a cascade of n states. The purpose of these cascades is to introduce a range of probabilities for transitions between the weak and strong states. This is analogous to the factor q introduced previously, except that, in this case, a sequence of n different transition probabilities, q_i for $i = 1, 2, \dots, n$, is included. Specifically, whenever the conditions for synaptic strengthening are met, which occurs at a rate f_+r , a synapse in state i of the weak cascade makes a transition to state 1 of the strong cascade with probability q_i (green arrows pointing up and to the right in Figure 2). Similarly, whenever the conditions for synaptic weakening are met, which occurs at a rate f_-r , a synapse in state i of the strong cascade makes a transition to state 1 of the weak cascade with the same probability q_i (red arrows pointing up and to the left in Figure 2). To achieve a wide range of transition rates, we arrange these different probabilities in a geometric sequence, so that $q_i = x^{i-1}$ for $i =$

$1, 2, \dots, n - 1$. To compensate for the boundary effects that occur for the last state in the cascade, we set $q_n = x^{n-1}/(1-x)$, although this adjustment is convenient rather than essential (see Experimental Procedures). The value of x is taken to be $1/2$ for reasons explained below.

The transitions described in the previous paragraph correspond to synaptic plasticity that changes the strength of a synapse from weak to strong (LTP-type events) or strong to weak (LTD-type events). In addition, there are metaplastic transitions in the model between the states in a given cascade. These do not change the strength of the synapse but, instead, push it to lower cascade levels (higher i values). Specifically, whenever the conditions for synaptic strengthening are met, a synapse in state i of the strong cascade makes a transition to state $i + 1$ of the strong cascade with probability p_i^+ (green arrows pointing down in Figure 2). Similarly, whenever the conditions for synaptic weakening are met, a synapse in state i of the weak cascade makes a transition to state $i + 1$ of the weak cascade with probability p_i^- (red arrows pointing down in Figure 2). For most of the examples shown below, the metaplastic transition probabilities are the same and given by $p_i^\pm = x^i/(1-x)$.

At this point, the structure of the cascade model and the values of its parameters [setting $x = 1/2$ or $p_i^\pm = x^i/(1-x)$, for example] may appear arbitrary. Here, we will provide a heuristic justification for the various choices being made and then address this issue more rigorously in a later section on optimization. Cascades of states with progressively lower probabilities of transition provide a combination of labile states (those with small i values) to enhance the initial amplitude of the memory signal and states resistant to plasticity (those with large i values) to increase memory lifetimes. The cascade performs best if all of its states are equally occupied so that the full range of transition probabilities is equally available. When potentiation and depression are balanced ($f_+ = f_-$), the choice of the metaplastic transition probabilities $p_i^\pm = x^i/(1-x)$ assures that, at equilibrium, the different cascade states are equally occupied (see Experimental Procedures). We discuss what happens in the unbalanced state ($f_+ \neq f_-$) in a later section. With equal occupancy, however, the amplitude of the initial memory signal, which relies primarily on a few of the most labile states at the top of the cascade, is proportional to $1/n$, the inverse of the number of states in the cascade. This makes it important to keep the cascade as small as possible, and having plasticity transition probabilities q_i that grow exponentially is a way of obtaining a large range of transition rates without introducing too many states. In a later section, we will discuss the optimality of this choice. Furthermore, the value of $1/2$ for x is the largest value consistent with maintaining $p_1^\pm \leq 1$, so choosing this value gives the maximum range of transition probabilities with the smallest number of cascade states. Finally, it is important to “reset” the cascade so that synapses do not keep progressing to lower levels (large i values) and becoming highly resistant to further plasticity. This reset is provided by terminating all the plasticity transitions at the top ($i = 1$) level of the target cascade.

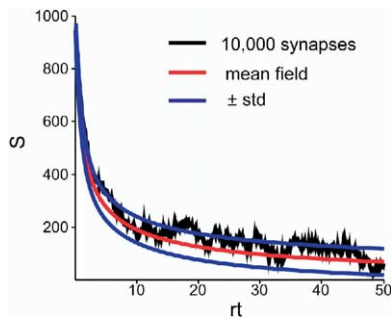


Figure 3. Memory Signal as a Function of Time following Storage of a Memory Trace

The black curve shows the memory signal obtained from simulating 10,000 synapses described by the cascade model of Figure 2, except with ten states per cascade. The red curve is the value obtained from a mean-field calculation, and the blue lines indicate one standard deviation away from this curve.

The black line in Figure 3 shows a sample run involving 10,000 synapses, each described by a cascade model with $n = 10$ states. The synapses were initialized in a random configuration drawn from the equilibrium distribution. This means that each synapse was randomly assigned to be either strong or weak and then placed randomly (with equal probability) into one of the $n = 10$ states in the appropriate cascade. At time 0, half the synapses were subject to a candidate potentiation event and half to a candidate depression. For the synapses subject to candidate potentiations, this means that synapses in weak state i made transitions to strong state 1 with probability q_i , and synapses in strong state i made transitions to strong state $i + 1$ with probability p_i^+ . The corresponding transitions were also made for synapses subject to candidate depression events. After that, the synapses were subject to random candidate potentiation and depression events at rates f_+r and f_-r with $f_+ = f_- = 1/2$ (the rate r does not need to be specified because it sets the unit of time in all our simulations). The signal being plotted is determined by dividing the synapses into two groups, those potentiated by memory storage and those depressed by memory storage. For the first group, we compute the number of synapses that are in the strong state minus the number that were in the strong state prior to memory storage. For the second group, we compute the number of synapses that are in the weak state minus the number that were in the weak state prior to memory storage. Because the difference in strength between the weak and strong states in these simulations is defined to be 1 and $f_+ = f_-$, the memory signal is simply the sum of these two terms. The memory signal following a memory storage at time 0 is indicated by the black line in Figure 3. The jagged wiggles in this curve arise from the random nature of the ongoing plasticity. The trend of the curve is a decrease toward baseline that is of a power-law rather than exponential form. In particular, note that long tail at small values that are nevertheless significantly different from zero.

Simulations like that used to generate the black curve in Figure 3 are time consuming, especially if large

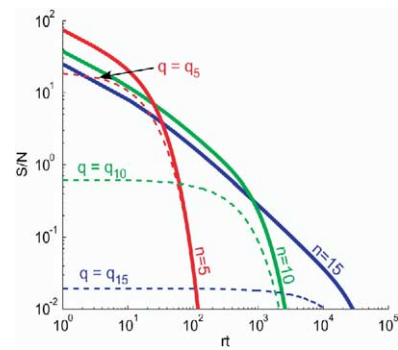


Figure 4. Signal-to-Noise Ratio as a Function of Time

Decay of the signal-to-noise ratios of memory traces stored by cascade models of different sizes (solid curves) and binary models with different transition probabilities (dashed curves). The solid curves for the cascade models initially decay as a power-law, but this changes to an exponential decay at a time determined by the smallest transition probability q_n in the model. Increasing n , and hence decreasing $q_n = 2^{-n+1}$, expands the range over which the power-law applies. The binary models shown have transition probabilities set to the minimum transition probability in the $n = 5, 10$, and 15 cascade models (red, green, and blue curves, respectively). All these curves correspond to memory storage with 10^5 synapses.

numbers of synapses are being considered. Fortunately, a statistical “mean-field” analysis of the dynamics of plasticity in the cascade model can reproduce the results of the multisynapse simulation quite accurately in a fraction of the time. The equations of the mean-field approach are given in the Experimental Procedures section. The red line in Figure 3 shows the memory signal predicted by the mean-field equations, and the blue lines indicate plus and minus one standard deviation from this. The mean-field results describe the mean and standard deviation of the black curve for 10,000 synapses quite well, and the accuracy increases as more synapses are considered. For this reason, all the results we report below come from analysis and simulation of the mean-field equations.

Model Results

As stated previously, a major point in constructing a cascade model of synaptic plasticity is to obtain a power-law decay of the memory trace over time. To track the memory trace, we plot its signal-to-noise ratio over time in Figure 4. The initial segments of all three curves in Figure 4 show a decay proportional to $t^{-3/4}$. Eventually, these curves make a transition to an exponential decay. This occurs when q_nrt is of order 1. In other words, the power-law decay is limited by the size of the smallest plasticity transition probability in the cascade. As the number of elements in the cascade increases, the power-law behavior extends over a larger time interval, as seen by comparing the different solid curves in Figure 4. The extension of the range of the power-law behavior is accompanied by a reduction in the initial signal-to-noise ratio. The initial signal-to-noise ratio is proportional to $1/n$, but note that a small increase in n results in a large increase in the range over which a power-law decay applies. This is because

$q_n = 2^{-n} + 1$, so the minimum transition probability decreases exponentially with increasing n . Equivalently, the cascade size n and the initial memory signal amplitude, which is proportional to $1/n$, both vary only logarithmically as a function of q_n or, equivalently, as a function of the maximum memory lifetime (see Figure 1).

The dashed curves in Figure 4 show a comparison of the performance of the cascade model with the noncascade binary model discussed earlier (equivalent to an $n = 1$ cascade model with $q_1 = q$). To make the comparison as fair as possible, we show signal-to-noise ratio curves for noncascade binary models with transition probabilities that match the minimum transition probability in each of the cascade models shown in Figure 4. In other words, we set $q = q_n = 2^{-n} + 1$ for $n = 5, 10$, and 15 . It is clear from Figure 4 that the cascade models vastly outperform their noncascade counterparts. Note, in particular, that only the binary model with $q = q_5$ in Figure 4 has an initial signal-to-noise ratio larger than 1.

We define the memory lifetime as the point on the curves of Figure 4 when the signal-to-noise ratio of the memory trace goes to 1. The key to getting improved memory lifetimes from the cascade model is to assure that the “break” in the curves where power-law behavior gives way to exponential decay occurs later in time than the point at which the signal-to-noise ratio goes to 1. In the example of Figure 4, the $n = 5$ cascade does not satisfy this condition, while the $n = 10$ and $n = 15$ cascades do. This means that for memories stored using 10^5 synapses, $n = 5$ is too small, $n = 10$ is optimal, and $n = 15$ is too large because over the relevant range where the signal-to-noise ratio is larger than 1, it has a lower signal-to-noise value than the $n = 10$ model.

We can determine the optimal size of the cascade for a particular memory application by using an analytic fit to the signal-to-noise curves in Figure 3. Over the power-law portion, before the exponential fall-off occurs, these curves are well fit by the formula

$$\frac{S}{N} = \frac{12\sqrt{N_{\text{syn}}}}{5n(1 + (rt)^{3/4})} \quad (1)$$

Assuming the number of synapses is large, this is equal to 1 at the time

$$t_{\text{max}} = \left(\frac{12}{5n}\right)^{4/3} \frac{N_{\text{syn}}^{2/3}}{r} \quad (2)$$

but this is only the correct memory lifetime if the condition $q_n r t_{\text{max}} = 2^{-n} + 1 r t_{\text{max}} < 1$ is satisfied. Combining these results, we obtain a condition on the number of states in the cascade,

$$n + \frac{4}{3} \log_2(n) > 1 + \frac{4}{3} \log_2(12/5) + \frac{2}{3} \log_2(N_{\text{syn}}). \quad (3)$$

The smaller n is, within the constraints of this bound, the larger will be the amplitude of the memory signal. Although the optimal value of n depends on the number of synapses used to store the memory, this dependence is weak (only logarithmic), so no precise tuning of the cascade is required to achieve near-optimal performance.

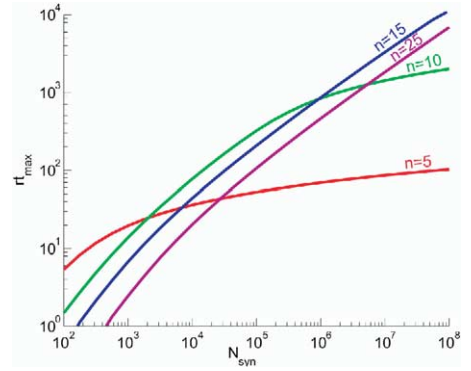


Figure 5. Dependence of Memory Lifetime on Synapse Number
Memory lifetime (in units of $1/r$) for different size cascade models versus the number of synapses used in storage. The optimal number of cascade states depends on the number of synapses being used for memory storage.

The relationship between memory lifetime and the number of synapses used to store the memory is elaborated further in Figure 5. For 1000 synapses, the optimal model has $n = 5$, while for 10^6 synapses the optimal model has $n = 15$. The key point, however, is that over wide ranges in the number of synapses, these models show a power-law relationship between the memory lifetime and the number of synapses used in storage. As stated above, the relationship is $t_{\text{max}} \sim N_{\text{syn}}^{2/3}$ (see Equation 2 above).

Up to now, we have considered a balanced situation, in which the rates of synaptic potentiation and depression are equal, $f_+ = f_- = 1/2$. We noted above that in this balanced situation, it is possible to increase memory lifetimes quite dramatically (by a factor of m^2 for m states) by increasing the number of allowed levels of synaptic strength, even in a noncascade configuration. The problem is that this improvement is greatly diminished if the effects of synaptic potentiation and depression are not balanced. This is shown in Figure 6A. In the remaining panels of Figure 6, we explore the effects of unbalanced plasticity (when $f_+ \neq f_-$) on memory lifetimes in the cascade model. The percentages in Figure 6 refer to the quantity $f_+ - f_-$. Thus, 0% corresponds to the balanced case already discussed, 25% means that $f_+ = 0.625$ and $f_- = 0.375$, and 50% refers to $f_+ = 0.75$ and $f_- = 0.25$. The results are identical if the values of f_+ and f_- are interchanged.

Figure 6B illustrates what happens if we change the balance between potentiation and depression events in the cascade model, which have been equal in all the examples shown up to this point. Memory lifetimes clearly diminish when potentiation and depression are unbalanced, but the effect for the $n = 15$ cascade model shown is much less severe than that shown in Figure 6A for an $m = 15$ level noncascade model. Importantly, the power-law increase of the memory lifetime as a function of the number of synapses is not destroyed by an unbalanced situation. The cascade model is thus robust, but not unaffected, by an imbalance in the relative amounts of potentiation and depression.

The model shown in Figure 6B has the metaplasticity

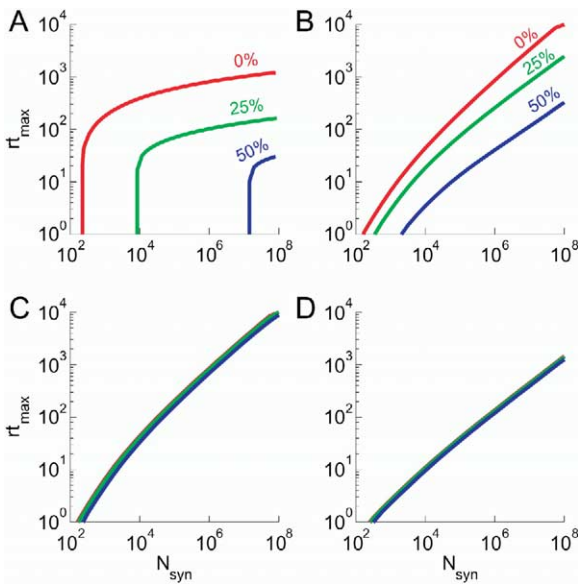


Figure 6. The Effects on Memory Lifetime of Changing the Balance between Potentiation and Depression of Synapses

The percentages in (A) and (B) refer to the difference between the probabilities of potentiation and depression, $f_+ - f_-$. (A) Results for a noncascade model with 15 levels of synaptic strength. (B) Results for a 15-state cascade model without any parameter adjustment. (C) Results for a 15-state cascade model with optimal parameter tuning. (D) Results of a modified 15-state cascade model without any parameter tuning (see text).

probabilities set to $p_i^\pm = x^i / (1 - x)$, which is the optimal relationship for the balanced case when $f_+ - f_- = 0$. The primary reason that the unbalanced curves in Figure 6B show poorer performance is that the different cascade states are not equally occupied when this choice of metaplasticity transition probabilities is used and $f_+ - f_- \neq 0$. For the unbalanced case, the formula for these probabilities that leads to uniform occupancies of the cascades states is $p_i^\pm = f_\pm x^i / (f_\pm(1 - x))$ (see [Experimental Procedures](#)). It is reasonable to assume that cascade transition probabilities would be optimized for the prevailing level of imbalance in the relative amounts of potentiation and depression. In Figure 6C, we show what happens if this adjustment is made [in other words, for this panel, we set $p_i^\pm = f_\pm x^i / (f_\pm(1 - x))$ rather than $p_i^\pm = x^i / (1 - x)$ as in panel B]. There is virtually no effect of unbalancing potentiation and depression if this adjustment is made.

The fact that the optimal formula of the metaplastic transition probabilities is given by $p_i^\pm = f_\pm x^i / (f_\pm(1 - x))$ can be interpreted in an interesting way that would allow the synapse to make the adjustment to the prevailing level of plasticity imbalance automatically. Up to now, we have assumed that the metaplastic transitions that move a synapse down the “+” cascade from state i , occurring with probability p_i^+ , are the result of candidate potentiation events, which take place at a rate $f_+ r$. Similarly, transitions down the “-” cascade take place with probability p_i^- and arise from candidate depression events occurring at the rate $f_- r$. The rates for these two types of transitions are thus $p_i^\pm f_\pm r$. Substituting into

this the equation for the optimally adjusted metaplastic transition probabilities, $p_i^\pm = f_\pm x^i / (f_\pm(1 - x))$, we find that these rates are given by $f_\pm r x^i / (1 - x)$. This is equivalent to what we would obtain from noncompensated transition probabilities $p_i^\pm = x^i / (1 - x)$ if metaplastic transitions in the + and - cascades were triggered by candidate depression and potentiation events, respectively, rather than the other way around. In other words, in this alternative scheme candidate potentiation events drive transitions down the weak cascade of states and candidate depression events drive transitions down the strong cascade. As seen in Figure 6D, this scheme allows memory lifetimes to be almost totally independent of the state of balance between potentiation and depression events without parameter tuning, but at the expense of a somewhat smaller memory signal. The reduction in the size of the memory signal is due to the fact that the “backward” metaplastic transitions in the alternative model have a negative impact on the initial storage of the tracked memory. In addition, this form of metaplasticity does not allow the synapse to react optimally to correlated sequences of plasticity events. For these reasons, we do not favor this scheme, but we felt it worthwhile to point out its self-adjusting property.

Model Optimization

As mentioned previously, we made a number of choices in constructing the cascade model that may seem fairly arbitrary. For example, we set the plasticity transition probability for state i equal to $q_i = 2^{-i} + 1$, and we set the cascade transition probabilities so that the different states would be equally occupied at equilibrium. In this section, we make two statements about these choices. First, we show that they produce near-optimal performance. Second we show that similar performance can be obtained for a wide range of related models, indicating that the cascade scheme is robust and does not require fine-tuning.

We mentioned previously that a binary model can either achieve an initial signal-to-noise ratio or a maximum lifetime proportional to the square root of the number of synapses ($S_0 / N_0 \propto \sqrt{N_{\text{syn}}}$ or $t_{\text{max}} \propto \sqrt{N_{\text{syn}}}$), but not both. We now show that the cascade model comes very close (to within a logarithmic factor) of achieving the goal of making both quantities proportional to the square root of the number of synapses.

The signal-to-noise ratio in the cascade model starts to fall off exponentially with time, rather than as a power, at a time proportional to $1/q_n$, the inverse of the minimal transition probability in the model. Requiring the signal-to-noise ratio to be greater than 1 at this point, introduces the requirement that $q_n \propto 1 / \sqrt{N_{\text{syn}}}$. This means that the maximum memory lifetime in the cascade model has the same dependence as in the binary model with small q , that is, $t_{\text{max}} \propto \sqrt{N_{\text{syn}}}$. The signal-to-noise ratio, however, is almost as large in the cascade model as it is in the $q = 1$ version of the binary model. The initial signal-to-noise ratio in the cascade model satisfies $S_0 / N_0 \propto \sqrt{N_{\text{syn}}} / \ln(1 / q_n)$, which means that $S_0 / N_0 \propto \sqrt{N_{\text{syn}}} / \ln(\sqrt{N_{\text{syn}}})$. Thus, the initial signal-to-noise ratio is only a logarithmic factor smaller than it is in the $q = 1$ model, meaning that the cascade model comes close to matching the best features of both extreme versions of the binary model.

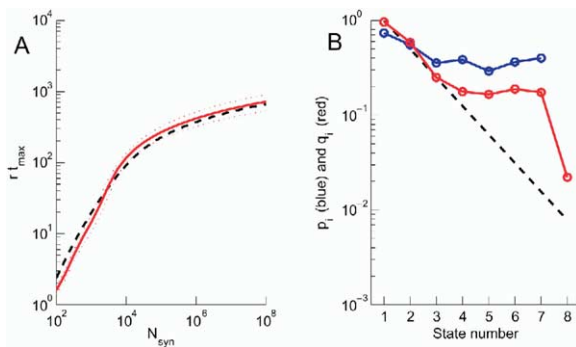


Figure 7. The Monte Carlo Solution versus the Cascade Model
(A) Memory lifetime versus the number of synapses for an $n = 8$ cascade model (black dashed curve) compared with the average of 100 Monte Carlo optimized models (red curve). Red dots denote plus and minus one standard deviation across this sample. (B) Transition probabilities for different cascade states for the cascade model (black dashed line) compared to the average parameters of the Monte Carlo optimized model. The red points represent the weak-strong transition probabilities (q_i), and the blue lines are the within cascade transition probabilities (p_i). The vertical axis has a logarithmic scale to expose the exponential decay of the transition probabilities.

To continue exploring the issue of optimality, we studied a model in which initially random parameters were varied by a Monte Carlo procedure to maximize the memory lifetime. Because we restricted this analysis to the symmetric case $f_+ = f_-$, we set the downward transition probabilities p_i to the same values for both the weak and strong cascades. The Monte Carlo procedure randomly perturbs all the cascade transition probabilities p_i and q_i by multiplying them by random factors and accepts only those modifications that increase the memory lifetime. The optimal cascade transition probabilities depend, in general, on the number of synapses and on the size of the cascade. For a specific number of states, the memory lifetime is maximal over a limited range in the number of synapses. The upper bound of this range is determined by the memory lifetime at which the power law breaks down. For example, the model with $n = 10$ is optimal up to a memory lifetime of $rt_{\max} = 2^9 = 512$ and up to roughly 3×10^5 synapses. When the memory lifetime is maximized for one particular number of synapses N_{syn} and a given size of the cascade, the memory lifetime of the Monte Carlo solution is slightly better than the model solution, but only over a small interval around N_{syn} in the number of synapses and at the expense of a smaller initial signal-to-noise ratio. Outside this region, the Monte Carlo solution performs poorly. We next modified the Monte Carlo procedure so that it accepted only those changes that improve the memory lifetime over a given range of N_{syn} . As this range is extended, the performance of the Monte Carlo-optimized model approaches that of the cascade model, as shown in Figure 7.

The performance curve in Figure 7A showing the memory lifetime versus the number of synapses of the cascade model with $n = 8$ states is well approximated by the optimal solution found by the Monte Carlo pro-

cedure. The Monte Carlo model performs slightly better than the cascade model for large numbers of synapses (at the expense of a smaller initial signal-to-noise ratio) and slightly worse for small numbers of synapses. Although the Monte Carlo procedure starts from completely random cascade transition probabilities, the final transition probabilities are similar to those of the cascade model for the more plastic states in the cascade (small i), but are larger for less plastic states (Figure 7B). This indicates that similar memory performance can be achieved with a variety of parameter values. Strict adherence to the geometric series is not essential.

Analysis of a large number of Monte Carlo runs revealed the following general features. (1) No Monte Carlo solution had a longer memory lifetime over the entire range of N_{syn} considered, which was $10^2 \leq N_{\text{syn}} \leq 10^8$. (2) When the Monte Carlo solution produced a longer memory lifetime than the cascade model over a limited range of N_{syn} , as it sometimes did, the maximal improvement was about 30%. (3) Sometimes the memory lifetime of the Monte Carlo solution exceeded that of the cascade model for N_{syn} greater than a certain value. This value was always in the range where the signal-to-noise ratio of the cascade model was exponentially decaying before it reached the value 1, that is, in a range where the model is not intended to operate. (4) The Monte Carlo procedure revealed many solutions with similar performance curves but different transition probabilities. In this regard, it is relevant to point out that Figure 7B shows averages over 100 Monte Carlo runs. The individual solutions from these runs showed considerably larger variations in their parameter values than these averages, including potential “inversion” in which the probabilities do not decrease monotonically with state number. These features indicate that the cascade model provides an optimal range of performance but that its parameter values are by no means unique as a means of achieving such performance.

Discussion

We propose that memories are retained through the modification of synaptic strength in a more complex manner than the simple switch-like picture that has dominated thinking about the synaptic basis of memory. Synapses that are modified by activity in a switch-like manner are not capable of supporting ongoing storage and retention of memory at anywhere near the capacities seen in animals and humans. The demands of ongoing memory storage require synapses that show a wide range of degrees of plasticity linked by metaplastic transitions. We have constructed one such model and shown that it significantly out-performs the standard alternatives. In building the model, we made some parameter choices that we have argued optimize memory performance. As results from the Monte Carlo procedure demonstrate (Figure 7), memory performance is robust to changes in these parameters, and it degrades gracefully as they are varied. Thus, the model does not require fine-tuning to work well.

The key element in the cascade models we have

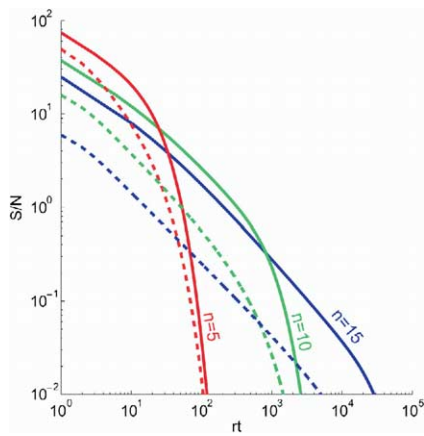


Figure 8. Signal-to-Noise Ratios as a Function of Time
A comparison of the time-evolution of the signal-to-noise ratio of the memory signal for different size cascade models (solid curves) with models in which noncascade binary synapses take a range of q values (dashed curves). For each noncascade model, synapses take the same range of values across the population as in they do for each individual synapses in the corresponding cascade model, which is represented by the same colored curve.

studied is the fact that synapses can exist in states that are highly plastic or that are resistant to plasticity. In this model, all the synapses have the same structure, with each synapse possessing the full range of plasticities. Another way of achieving a range of plasticities would be to have a heterogeneous population of synapses, each with a different degree of plasticity. In other words, a population of synapses could be described by a binary model with a range of different transition probabilities q across the population. Such a scheme can produce memory signals with power-law decay. However, as shown in **Figure 8**, this distributed scheme does not perform nearly as well as the cascade model we have been studying. The pairs of different colored curves in **Figure 8** show the original cascade model, with states having transition probabilities ranging from q_n to 1 (for $n = 5, 10,$ and 15), and a corresponding heterogeneous binary model in which each synapse is characterized by a single transition probability, but the transition probabilities for different synapses range from the same q_n (for $n = 5, 10,$ and 15) to 1. The distribution of q values over this range has been chosen so that the performance of the heterogeneous binary model matches that of the corresponding cascade model as closely as possible (this comes about when the distribution is proportional to $q^{-5/4}$). Nevertheless, the cascade model outperforms the heterogeneous binary model in all cases. This is because the cascade model allows correlations in the pattern of potentiation and depression events at a single synapse to affect the degree of plasticity, whereas the heterogeneous binary model does not. For example, in the cascade model, synapses that are frequently potentiated become more resistant to further changes, in particular to depression. In the heterogeneous binary model, each synapse is stuck with a fixed transition probability that is unaffected by its history of modification.

Part of the difference in performance seen in **Figure 8** is due to the size of the initial signal-to-noise ratio in the two models. As stated previously, the initial signal-to-noise ratio in the cascade model is proportional to 1 over the number of cascade states or, equivalently, to 1 over the logarithm of the minimum transition probability, q_n . For the heterogeneous binary model, the initial signal-to-noise ratio for the distribution we have used is proportional to $q_n^{1/4}$. This is better than the q_n dependence of the ordinary binary model, but not as good as the weak logarithmic dependence of the cascade model.

The cascade model makes some direct and testable predictions about the nature of synaptic plasticity and its relationship to memory storage. First, the model predicts that when a synapse is repeatedly subject to long-term potentiation or depression, it should not keep changing its strength, but rather should become more resistant to further plasticity. For example, a synapse that is repeatedly potentiated to the point where it is not becoming any stronger should become more resistant to subsequent depotentiation protocols than a synapse that is potentiated to the same degree by a single tetanization. Furthermore, each repeated tetanization should make the synapse more resistant to depotentiation. Finally, after depotentiation, the synapse should return to a state exhibiting a more labile form of plasticity. Similar statements apply to long-term depression. Some evidence exists that this is in fact the case (D.H. O'Connor et al., 2003, Soc. Neurosci., abstract). At the behavior end of the spectrum, **Pavlik and Anderson (2005)** have argued on the basis of psychophysical data that the memory lifetime changes as a function of training history in a manner similar to what we have proposed for synaptic efficacy.

Another prediction that arises from the model concerns sensory deprivation experiments, which are often used to study the effects of activity on synaptic plasticity. The model predicts that sensory deprivation should enhance plasticity within a deprived region, whereas high levels of activity should reduce plasticity. This could be tested, for example, by studying synaptic plasticity in slices from deprived and nondeprived areas. Modification of plasticity due to sensory deprivation has been observed (**Allen et al., 2003**), but this may be due to saturation effects distinct from the mechanism we propose.

We have considered ongoing memory for everyday occurrences rather than, for example, single-trial learning arising from a dramatic event. It is easy to see, however, how the cascade model could give rise to long-lasting memories arising from a single isolated experience. The key to switching the model from ongoing to single-trial memory would be the presence of a neuromodulator that increases the metaplastic transition probabilities p_i^\pm in response to the stress or other impact of an exceptional experience. If these probabilities are modulated to values near 1, the synapse will rapidly move to states deep within the cascade (states with large i values) that are highly resistant to further plasticity. In this way, a long-lasting memory trace that would normally be formed in a small number of synapses over an extended period of time due to rare metaplastic

transition could be formed virtually instantaneously in many synapses.

The cascade model could also provide interesting dynamics for reward-based learning. A problem with reward-based schemes of synaptic modification is that the reward often arrives a considerable time after the activity that produced the rewarded behavior. Synaptic changes induced by the initial activity must therefore be retained temporarily and then either removed or elevated to longer-lasting forms, depending on whether a punishment or a reward results. The cascade model provides exactly such an arrangement because its more labile states provide temporal storage, and reward-based modulation could gate more permanent storage for rewarded actions by increasing the transition probability to less plastic states.

Because of its rich dynamics, the cascade model opens up the possibility of accounting for a number of temporal effects in learning and memory. A prominent one is the difference in memory performance and long-term synaptic potentiation between massed and spaced training paradigms (Mauelshagen et al., 1998; Hermitte et al., 1999; Menzel et al., 2001; Wu et al., 2001; Sutton et al., 2002; Scharf et al., 2002; Woo et al., 2003; Zhou et al., 2003). It is relatively easy to incorporate this feature into cascade models. The key to forming long-lasting memories in the cascade model is to force synapses into states deep within the cascade that are resistant to further plasticity. We treated the metaplastic transitions within each cascade as instantaneous, but it is likely, given that they are low-probability events, that a considerable time may be required to complete some of these transitions. If so, it would be important to delay further attempts at inducing metaplastic transitions until a previous transition is completed if the synapse is to be driven through a number of such transitions sequentially. In this way, the advantage of spaced over massed training arises quite naturally in these models.

Cascade models could potentially exhibit an interesting aging phenomenon. In the examples shown, the population of synapses was loaded initially into cascade states in a random manner with an equal distribution across states. This is the equilibrium configuration for a “mature” population of synapses. If, however, early in development, synapses started in states at the top of the cascade and then migrated to lower states during the aging process, we would expect to see a high degree of plasticity with few long-lasting memory traces early on and then less labile plasticity and more long-lasting traces later. The developmental trend is logarithmic in time, meaning that changes occur at a rate inversely proportional to age.

Although the molecular pathways relevant to synaptic plasticity have been studied intensely, little theoretical work has been done to illuminate our understanding of the collective role of these multiple pathways in memory storage. Genetic and pharmacological manipulations have induced a variety of plasticity and memory deficits characterized by complex temporal dynamics over a wide range of timescales (Malenka, 1991; Tully et al., 1994; Ghirardi et al., 1995; Sutton et al., 2001; Sanna et al., 2002). This array of forms of plasticity is precisely what we are modeling using a cascade

structure. We feel that, for describing memory processes, it is more important to capture this range of forms and timescales in a model than it is to capture any single form in detail. We propose that the numerous biochemical reactions and pathways underlying synaptic plasticity are there to support multiple-timescale, power-law plasticity. We suggest that this is a way for a system that must retain memories in the face of ongoing plasticity to take advantage of the large number of synapses in neural circuitry. This suggests that the abundance of molecular players underlying long-term plasticity is not merely a result of the vagaries of evolution. Rather, there has been evolutionary pressure to add additional elements to these biochemical cascades because their complexity is an essential feature required to make memory work.

Experimental Procedures

In the mean-field approach, a population of synapses is represented by a set of occupancies F_i^\pm that indicate the average fraction of synapses in state i of the “+” or “-” cascade, respectively. By definition,

$$\sum_{i=1}^n (F_i^+ + F_i^-) = 1.$$

The equations satisfied by the state occupancies can be derived using standard methods. They are

$$\frac{dF_i^+}{dt} = r \left(f_{\pm} \sum_{j=1}^N q_j F_j^- - (f_{\pm} p_i^+ + f_{\pm} q_i) F_i^+ \right), \quad (4)$$

$$\frac{dF_i^-}{dt} = r (f_{\pm} p_{i-1}^- F_{i-1}^- - (f_{\pm} p_i^- + f_{\pm} q_i) F_i^-), \quad (5)$$

for $1 < i < n$, and

$$\frac{dF_n^\pm}{dt} = r (f_{\pm} p_{n-1}^\pm F_{n-1}^\pm - f_{\pm} q_n F_n^\pm). \quad (6)$$

These equations reflect the fact that the rate of change in the occupancy of a particular state is given by adding up the rates at which that state is entered from other states and subtracting the rate at which transitions occur out of the state.

In addition, at the time of storage of the tracked memory, we make the discrete transformations

$$F_i^+ \rightarrow F_i^+ + \sum_{j=1}^N q_j F_j^- - p_i^+ F_i^+ \quad \text{and} \quad F_i^- \rightarrow F_i^- - q_i F_i^- \quad (7)$$

as well as

$$F_i^+ \rightarrow F_i^+ + p_{i-1}^+ F_{i-1}^+ - p_i^+ F_i^+, \quad (8)$$

for $1 < i < n$, and

$$F_n^+ \rightarrow F_n^+ + p_{n-1}^+ F_{n-1}^+ \quad (9)$$

for synapses being potentiated, and

$$F_i^- \rightarrow F_i^- + \sum_{j=1}^N q_j F_j^+ - p_i^- F_i^- \rightarrow F_i^- - q_i F_i^- \quad (10)$$

as well as

$$F_i^- \rightarrow F_i^- + p_{i-1}^- F_{i-1}^- - p_i^- F_i^-, \quad (11)$$

for $1 < i < n$, and

$$F_n^- \rightarrow F_n^- + p_{n-1}^- F_{n-1}^- \quad (12)$$

for synapses being depressed. This is equivalent to generating the transitions described by Equations 4–6 in one sudden jump.

The equilibrium occupancies from Equations 4–6 are obtained

by setting the right sides of these equations to 0, which gives

$$F_{i-1}^{\pm} = \left(\frac{f_{\pm} p_i^{\pm} + f_{\mp} q_i}{f_{\pm} p_{i-1}^{\pm}} \right) F_i^{\pm},$$

for $1 < i < n$, and

$$F_{n-1}^{\pm} = \left(\frac{f_{\pm} q_n}{f_{\pm} p_{n-1}^{\pm}} \right) F_n^{\pm}.$$

The choices $q_i = x^{i-1}$, $q_n = x^{n-1}/(1-x)$, and $p_i^{\pm} = f_{\mp} x^i / (f_{\pm}(1-x))$ then assure that all the occupancies F_i^{\pm} take equal values at equilibrium. For many of the cases, we considered, $f_+ = f_-$ so the last formula reduces to $p_i^{\pm} = x^i / (1-x)$

The level of noise in the memory signal due to ongoing synaptic modifications is equal to the standard deviation of the fluctuations in the memory signal at equilibrium in the absence of an imposed memory. Therefore, to compute the noise for the signal-to-noise computation, we allow the state occupancies to equilibrate in the absence of the tracked memory and define

$$p_{\infty}^{\pm} = \sum_{i=1}^n F_i^{\pm}.$$

The noise is then defined as

$$\text{Noise} = \sqrt{N_{\text{syn}} p_{\infty}^+ p_{\infty}^-}.$$

The memory signal is defined by dividing synapses into those that are potentiated by the stored memory and those that are depressed by it. We denote the occupancies of these two groups by P_i^+ and D_i^+ , respectively, so that $F_i^+ = P_i^+ + D_i^+$. The equilibrium occupancies of these two groups prior to memory storage satisfy

$$\sum_{i=1}^n P_i^+ = f_+ p_{\infty}^+$$

and

$$\sum_{i=1}^n D_i^+ = f_- p_{\infty}^+$$

so that

$$\sum_{i=1}^n (P_i^+ + D_i^+) = f_+$$

and

$$\sum_{i=1}^n (D_i^+ + D_i^-) = f_-.$$

We define the difference in strength between the strong and weak states to be 1. The memory signal is then the sum of the excess number of memory-potentiated synapses in the + state and the excess number of memory-depressed synapses in the - state. This is given by

$$\text{Signal} = N_{\text{syn}} \left(\sum_{i=1}^n P_i^+ - f_+ p_{\infty}^+ + \sum_{i=1}^n D_i^- - f_- p_{\infty}^- \right)$$

The excess number of states compared to the equilibrium state is the same as that compared to the state prior to memory storage because we assume the system is at equilibrium at that time.

Monte Carlo Procedure

The Monte Carlo procedure explores the space of all possible cascade transition probabilities p_i and q_i to maximize the memory lifetime for several values of N_{syn} and a given cascade size ($n = 8$ in Figure 7). The transition probabilities are initially random and uniformly distributed between 0 and 1, although small initial probabilities are avoided to guarantee that the initial signal-to-noise ratio is larger than 1. Then, all the p_i and q_i are multiplied by random factors of the form $1 + \eta$, where η is a zero mean Gaussian distributed random variable. The width of the distribution is initially set to 0.025, but this width is multiplied by a factor 0.999 every time a new configuration of cascade transition probabilities is accepted.

After having perturbed the transition probabilities, the new configuration is evaluated by computing the memory lifetime with a mean-field approach: a set of different values of N_{syn} is prepared by starting from a minimal value and by multiplying this value progressively by a constant factor until it reaches a maximum value. For example, the Monte Carlo procedure used in Figure 7 maximized the memory lifetime at 20 points equally spaced on a logarithmic scale over the range $10^2 \leq N_{\text{syn}} \leq 10^6$. The final results of the Monte Carlo procedure are rather insensitive to the density of points. For each N_{syn} , the memory lifetime is evaluated and compared to the memory lifetime of the previous configuration. The new configuration is always accepted if all the memory lifetimes have been improved, and it is immediately discarded if there is no improvement. In the intermediate cases, the new configuration is accepted with a probability $1/(1 + \exp(-2c))$, where c is the average (across the different N_{syn} values) percentage change of the memory lifetime. After 500 consecutive iterations for which there is no acceptance, the run is terminated. This usually happens after thousands of iterations. The whole procedure is repeated 100 times, and averages of the resulting solutions have been plotted in Figure 7.

Acknowledgments

This research was supported by the Swartz Foundation, NIH grant MH58754, and an NIH Pioneer Award. Much of this work was done during a visit by S.F. to Brandeis University sponsored by Xiao-Jing Wang, whose generosity we gratefully acknowledge, and funded by NIH grants DA016455 (X.-J.W.) and MH58754 (L.F.A.) and by EU grant ALAVLSI (S.F.).

Received: August 16, 2004

Revised: November 12, 2004

Accepted: February 1, 2005

Published: February 16, 2005

References

- Abraham, W.C., and Bear, M.F. (1996). Metaplasticity: the plasticity of synaptic plasticity. *Trends Neurosci.* 19, 126–130.
- Abraham, W.C., Logan, B., Greenwood, J.M., and Dragunow, M. (2002). Induction and experience-dependent consolidation of stable long-term potentiations lasting months in the hippocampus. *J. Neurosci.* 22, 9626–9634.
- Ahissar, E., Vaadia, E., Ahissar, M., Bergman, H., Arieli, A., and Abeles, M. (1992). Dependence of cortical plasticity on correlated activity of single neurons and on behavioral context. *Science* 257, 1412–1415.
- Allen, C.B., Celikel, T., and Feldman, D.E. (2003). Long-term depression induced by sensory deprivation during cortical map plasticity in vivo. *Nat. Neurosci.* 6, 291–299.
- Amit, D.J. (1989). *Modeling Brain Function* (New York: Cambridge University Press).
- Amit, D., and Fusi, S. (1992). Constraints on learning in dynamical synapses. *Network* 3, 443–464.
- Amit, D., and Fusi, S. (1994). Dynamic learning in neural networks with material synapses. *Neural Comp.* 6, 957–982.
- Anderson, R.B. (2001). The power law as an emergent property. *Mem. Cognit.* 29, 1061–1068.
- Barnes, C.A. (1979). Memory deficits associated with senescence: a neurophysiological and behavioral study in the rat. *J. Comp. Physiol. Psychol.* 93, 74–104.
- Bi, G.-q., and Poo, M.-m. (1998). Activity-induced synaptic modifications in hippocampal culture, dependence on spike timing, synaptic strength and cell type. *J. Neurosci.* 18, 10464–10472.
- Bliss, T.V., and Collingridge, G.L. (1993). A synaptic model of memory: long-term potentiation in the hippocampus. *Nature* 361, 31–39.
- Bogacz, R., Brown, M.W., and Giraud-Carrier, C. (2001). Model of familiarity discrimination in the perirhinal cortex. *J. Comput. Neurosci.* 10, 5–23.

- Bredt, D.S., and Nicoll, R.A. (2003). AMPA receptor trafficking at excitatory synapses. *Neuron* 40, 361–379.
- Brown, M.W., and Xiang, J.Z. (1998). Recognition memory: neuronal substrates of the judgment of prior occurrence. *Prog. Neurobiol.* 55, 149–189.
- Fischer, T.M., Blazis, D.E., Priver, N.A., and Carew, T.J. (1997). Metaplasticity at identified inhibitory synapses in *Aplysia*. *Nature* 389, 860–865.
- Fu, Y.X., Djupsund, K., Gao, H., Hayden, B., Shen, K., and Dan, Y. (2002). Temporal specificity in the cortical plasticity of visual space representation. *Science* 296, 1999–2003.
- Fusi, S. (2002). Hebbian spike-driven synaptic plasticity for learning patterns of mean firing rates. *Biol. Cybern.* 87, 459–470.
- Ghirardi, M., Monterolo, P.G., and Kandel, E.R. (1995). A novel intermediate stage in the transition between short- and long-term facilitation in the sensory to motor neuron synapse of *Aplysia*. *Neuron* 14, 413–420.
- Grossberg, S. (1982). Processing of expected and unexpected events during conditioning and attention: a psychophysiological theory. *Psychol. Rev.* 89, 529–572.
- Hermite, G., Pedreira, M.E., Tomsic, D., and Maldonado, H. (1999). Context shift and protein synthesis inhibition disrupts long-term habituation after spaced, but not massed, training in the crab *Chasmagnathus*. *Neurobiol. Learn. Mem.* 71, 34–49.
- Hertz, J., Krogh, A., and Palmer, R.G. (1991). *Introduction to the Theory of Neural Computation* (Redwood City, CA: Addison-Wesley).
- Jenkins, J.G., and Dallenbach, K.M. (1924). Oblivescence during sleep and waking period. *Am. J. Psychol.* 35, 605–612.
- Larson, L.P., Xiao, P., and Lynch, G. (1993). Reversal of LTP by theta frequency stimulation. *Brain Res.* 600, 97–102.
- Malenka, R.C. (1991). Postsynaptic factors control the duration of synaptic enhancement in area CA1 of the hippocampus. *Neuron* 6, 53–60.
- Manahan-Vaughan, D., and Braunewell, K.H. (1999). Novelty acquisition is associated with induction of hippocampal long-term depression. *Proc. Natl. Acad. Sci. USA* 96, 8739–8744.
- Mauelshagen, J., Parker, G.R., and Carew, T.J. (1998). Differential induction of long-term synaptic facilitation by spaced and massed applications of serotonin at sensory neuron synapses of *Aplysia californica*. *Learn. Mem.* 5, 246–256.
- Menzel, R., Manz, F., and Greggers, U. (2001). Massed and spaced learning in honeybees: the role of CS, US, the intertrial interval, and the test interval. *Learn. Mem.* 8, 198–208.
- Nickerson, R.S. (1965). Short-term memory for complex meaningful visual configurations: A demonstration of capacity. *Can. J. Psychol.* 19, 155–160.
- O'Dell, T.J., and Kandel, E.R. (1994). Low-frequency stimulation erases LTP through an NMDA receptor-mediated activation of protein phosphatases. *Learn. Mem.* 1, 129–139.
- Pavlik, P.I., and Anderson, J.R. (2005). Practice and forgetting effects on vocabulary memory: An activation-based model of the spacing effect. *Cogn. Sci.*, in press.
- Petersen, C.C., Malenka, R.C., Nicoll, R.A., and Hopfield, J.J. (1998). All-or-none potentiation at CA3–CA1 synapses. *Proc. Natl. Acad. Sci. USA* 95, 4732–4737.
- Sanes, J.R., and Lichtman, J.W. (1999). Can molecules explain long-term potentiation. *Nat. Neurosci.* 2, 597–604.
- Sanna, P.P., Cammalleri, M., Berton, F., Simpson, C., Lutjens, R., Bloom, F.E., and Francesconi, W. (2002). Phosphatidylinositol 3-kinase is required for the expression but not for the induction or the maintenance of long-term potentiation in the hippocampal CA1 region. *J. Neurosci.* 22, 3359–3365.
- Scharf, M.T., Woo, N.H., Lattal, K.M., Young, J.Z., Nguyen, P.V., and Abel, T. (2002). Protein synthesis is required for the enhancement of long-term potentiation and long-term memory by spaced training. *J. Neurophysiol.* 87, 2770–2777.
- Shepard, R.N. (1967). Recognition memory for words, sentences, and pictures. *Journal of Verbal Learning and Verbal Behavior* 6, 156–163.
- Simons, D.J. (1996). In sight, out of mind: When object representations fail. *Psychol. Sci.* 7, 301–305.
- Standing, L. (1973). Learning 10,000 pictures. *Q. J. Exp. Psychol.* 25, 207–222.
- Standing, L., Conezio, J., and Haber, R.N. (1970). Perception and memory for pictures: Single-trial learning of 2500 visual stimuli. *Psychon. Sci.* 19, 73–74.
- Staubli, U., and Lynch, G. (1990). Stable depression of potentiated synaptic responses in hippocampus with 1–5 Hz stimulation. *Brain Res.* 513, 113–118.
- Sutton, M.A., Masters, S.E., Bagnall, M.W., and Carew, T.J. (2001). Molecular mechanisms underlying a unique intermediate phase of memory in *Aplysia*. *Neuron* 31, 143–154.
- Sutton, M.A., Ide, J., Masters, S.E., and Carew, T.J. (2002). Interaction between amount and pattern of training in the induction of intermediate- and long-term memory for sensitization in *Aplysia*. *Learn. Mem.* 9, 29–40.
- Tsodyks, M. (1990). Associative memory in neural networks with binary synapses. *Mod. Phys. Lett. B* 4, 713–716.
- Tully, T., Preat, T., Boynton, S.C., and Del Vecchio, M. (1994). Genetic dissection of consolidated memory in *Drosophila*. *Cell* 79, 35–47.
- Villarrreal, D.M., Do, V., Haddad, E., and Derrick, B.I. (2002). NMDA receptor antagonists sustain LTP and spatial memory: active processes mediate LTP decay. *Nat. Neurosci.* 5, 48–52.
- Walker, M.P., Brakefield, T., Hobson, J.A., and Stickgold, R. (2003). Dissociable stages of human memory consolidation and reconsolidation. *Nature* 425, 616–620.
- Willshaw, D. (1969). Non-holographic associative memory. *Nature* 222, 960–962.
- Wixted, J.T., and Ebbesen, E. (1991). On the form of forgetting. *Psychol. Sci.* 2, 409–415.
- Wixted, J.T., and Ebbesen, E. (1997). Genuine power curves in forgetting. *Mem. Cognit.* 25, 731–739.
- Woo, N.H., Duffy, S.N., Abel, T., and Nguyen, P.V. (2003). Temporal spacing of synaptic stimulation critically modulates the dependence of LTP on cyclic AMP-dependent protein kinase. *Hippocampus* 13, 292–300.
- Wu, G.-Y., Deisseroth, K., and Tsien, R.W. (2001). Spaced stimuli stabilize MAPK pathway activation and its effects on dendritic morphology. *Nat. Neurosci.* 4, 151–158.
- Xiao, M.Y., Nim, Y.P., and Wigstrom, H. (1996). Activity-dependent decay of early LTP revealed by dual EPSP recording in hippocampal slices from young rats. *Eur. J. Neurosci.* 9, 1916–1923.
- Xu, L., Anwyl, R., and Rowan, M.J. (1998). Spatial exploration induced a persistent reversal of long-term potentiation in rat hippocampus. *Nature* 394, 891–894.
- Zhou, Q., Tao, H.W., and Poo, M.-m. (2003). Reversal and stabilization of synaptic modifications in a developing visual system. *Science* 300, 1953–1957.